ELSEVIER

Journal of Alloys and Compounds 408–412 (2006) 608–612

Journal of ALLOYS AND COMPOUNDS

www.elsevier.com/locate/jallcom

Crystal structures and magnetic properties of double perovskite compounds Ca_2LnRuO_6 (Ln = Y, La–Lu)

Chiho Sakai*, Yoshihiro Doi, Yukio Hinatsu

Division of Chemistry, Graduate School of Science, Hokkaido University, Sapporo 060-0810, Japan

Received 30 July 2004; received in revised form 29 November 2004; accepted 15 December 2004

Abstract

The double perovskite compounds Ca_2LnRuO_6 (Ln = Y, La–Lu) have been prepared. The X-ray diffraction measurements show that Ca^{2+} and Ln^{3+} ions are partially disordered at the A site and half of the B site of the perovskite ABO_3, and that Ca^{2+}/Ln^{3+} and Ru^{5+} ions located at the B site are regularly ordered. Therefore, these compounds should be represented by $Ca_{2-x}Ln_x[Ln_{1-x}Ca_x]RuO_6$. The ratio of the Ln^{3+} ion located at the B site varies with its ionic radius. It is clear that the larger Ln ions occupy the A site and that the smaller Ln ions tend to occupy the B site.

Through magnetic susceptibility and specific heat measurements, it has been found that Ca_2LuRuO_6 shows an antiferromagnetic transition at 14 K.

Keywords: Double perovskite; Antiferromagnetic transition; Specific heat; Magnetic susceptibility

1. Introduction

The perovskite-type oxides have the general formula ABO_3, in which A represents a large metal cation and B represents a small one. The perovskite structure can be described as a framework of corner-shared BO_6 octahedra, which contain A cations at 12-coordinate sites. Double perovskite-type oxides have the formula $A_2B'B''O_6$, in which the primes indicate the different ions in different oxidation states, and B′ and B″ cations are regularly ordered, i.e. 1:1 arrangement of B′ and B″ ions has been observed over the six-coordinate B sites. Since the B cations generally determine the physical properties of perovskites, different kinds of B′ and B″ ion should show a variety of the physical properties of double perovskite oxides.

We have been studying the preparation, crystal structures and magnetic properties of double perovskite oxides containing Ru ion, Ba_2LnRuO_6 and Sr_2LnRuO_6, where Ln represents a rare earth ion [1–4]. The electronic structure of Ru^{5+} is $[Kr]4d^3$ (krypton electronic core [Kr]). Such highly oxidized cations from the second or third transition series sometimes show quite unusual magnetic behavior. So, the double perovskites Ba_2LnRuO_6 [1,2,5] and Sr_2LnRuO_6 [3–6] show interesting magnetic properties at low temperatures.

Now, our attention has been focused on double perovskite oxides in which A cation is Ca, Ca_2LnRuO_6. While the rare earth ion and ruthenium ion occupy B site in the above-mentioned two series of compounds, the situation is different when the A cation is Ca. For Ln = La and Nd, large Ln ion completely occupies the A site, while small Ln ion partly occupies its site for Ln = Y and Ho [7–9]. However, the crystal structure and magnetic properties of Ca_2LnRuO_6 including heavy rare earth ion have not been studied in detail yet.

In this study, we have prepared a series of Ca_2LnRuO_6 compounds (Ln = Y, La–Lu) and studied systematically their crystal structures by the powder X-ray diffraction, and investigated the magnetic properties of Ca_2LuRuO_6 through magnetic susceptibility and specific heat measurements.

---

* Corresponding author. Tel.: +81 11 706 2706; fax: +81 11 706 4931.
E-mail address: chi_phone726@ybb.ne.jp (C. Sakai).

0925-8388/$ – see front matter © 2005 Elsevier B.V. All rights reserved.
doi:10.1016/j.jallcom.2004.12.068

2. Experimental

Polycrystalline samples of Ca_2LnRuO_6 were prepared by firing the appropriate amounts of $CaCO_3$, Ln_2O_3 (Ln = La, Nd–Gd, Dy–Lu), Pr_6O_{11} or Tb_4O_7 and RuO_2, at 1373–1473 K for 12–100 h with frequent grindings and pelletings. X-ray powder diffraction measurements were performed on a Rigaku RINT 2100 diffractometer. The structure and lattice parameters were refined with a Rietveld program RIETAN 2000 [10].

Magnetic susceptibility measurements were performed under both the zero-field-cooled (ZFC) and field-cooled (FC) conditions with a SQUID magnetometer (Quantum Design MPMS model).

The specific heat measurements were carried out using a relaxation technique supplied by the commercial heat capacity measurement system (Quantum Design, Model PPMS). The sample in the form of a pellet (~10 mg) was mounted on an alumina plate with apiezon for better thermal contact. The specific heat and magnetic susceptibility were measured in the temperature range from 1.8 to 300 K.

3. Results and discussion

3.1. Crystal structure

The results of the X-ray diffraction measurements show that the title compounds Ca_2LnRuO_6 (Ln = Y, lanthanides) except for the Ce compound crystallize as the perovskite phase. For Ln = Ce, mixtures of the CeO_2, CaO and $CaRuO_3$ were generated, thus the Ca_2CeRuO_6 compound is excluded from this paper. Almost all compounds were obtained as a single phase. For Ln = Eu, Gd, Yb and Lu compounds, a small amounts of impurity phase (the C-type of Ln_2O_3 for Ln = Yb, Lu; unknown phase for Ln = Eu, Gd) was observed.

Fig. 1 shows the X-ray diffraction profile for Ca_2TbRuO_6. All the powder X-ray diffraction patterns for Ca_2LnRuO_6 were indexed with a monoclinic unit cell with space group $P2_1/n$. The X-ray diffraction profiles in low-angle region for all the compounds are plotted in the inset graph of Fig. 1. A marked difference in the intensity of some low-angle reflections was observed. The total intensity for (0 0 2) and (1 1 0) peaks is large for Ln = Y and Ho–Lu, while it is significantly small for Ln = La, Pr, Nd and Sm–Dy. If the A, B′ and B″ ions in the $A_2B'B''O_6$ compounds occupy the 4e (~0.5, ~0.5, ~0.25), 2c (0, 1/2, 0) and 2d (1/2, 0, 0) sites, respectively, the intensities of both peaks are approximately represented as $F(0\,0\,2 \text{ or } 1\,1\,0) \sim \pm(4f_A - 2f_{B'} - 2f_{B''} + \alpha f_O)$ ($f_A, f_{B'}, f_{B''}, f_O$ is the average atomic scattering factors at each site and α is the value determined by atomic positions of oxygen ions). Thus, this fact reflects that Ca^{2+} ions partially occupy the B′ or B″ sites for Ln = La, Pr, Nd and Sm–Dy compounds. In addition, the (0 1 1) and (1 0 1) peaks observed at $2\theta \sim 19°$ indicate the structural cation ordering between B′ and B″ sites [$F(0\,1\,1 \text{ or } 1\,0\,1) \sim \pm(2f_{B'} - 2f_{B''} + \alpha' f_O)$].

In order to clarify the exact cation distribution in this Ca_2LnRuO_6 series, the X-ray diffraction data were analyzed by the Rietveld method. The results of this analysis show that Ca^{2+} ions partially occupy the B′ site, i.e. the Ca_2LnRuO_6 is represented as $Ca_{2-x}Ln_x[Ln_{1-x}Ca_x]RuO_6$. In addition, they show that the B′ and B″ ions are regularly ordered in the NaCl-type. The B″ site is occupied by only Ru^{5+} ion and B′ site is randomly occupied by Ca^{2+} and Ln^{3+} ions. This result corresponds to the previous results on for Ca_2LnRuO_6 (Ln = La, Nd, Ho) reported by Battle et al. [7–9]. The crystal structure determined for Ca_2LnRuO_6 is illustrated in Fig. 2. The structural parameters for Ca_2LaRuO_6 and Ca_2LuRuO_6 are listed in Tables 1 and 2, respectively.

The variation of lattice parameters for Ca_2LnRuO_6 with Ln^{3+} radius is plotted in Fig. 3. The lattice parameters *a*, *b* and $c/\sqrt{2}$ trend to reduce with decreasing the Ln^{3+} ion size. How-

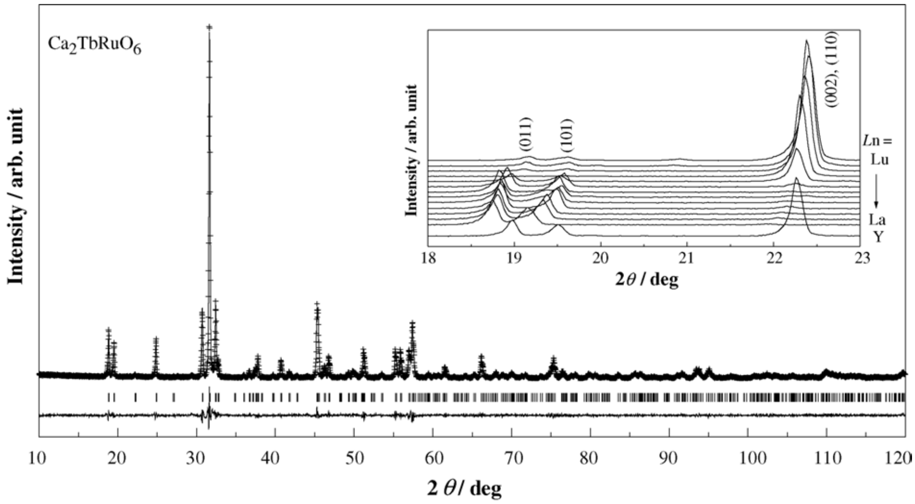

Fig. 1. X-ray diffraction profiles for Ca_2TbRuO_6. The X-ray diffraction profiles in the low-angle region for all the Ca_2LnRuO_6 compounds (Ln = La–Lu, Y) are plotted in the inset graph.

Table 1
Crystallographic data for Ca_2LaRuO_6

Atom	Site	Occupancy	*x*	*y*	*z*	B ($Å^2$)
Ca1	4e	0.5	0.5127(3)	0.5536(2)	0.2512(2)	0.55(3)
La1	4e	0.5	0.5127	0.5536	0.2512	0.55
Ru	2d	1.0	1/2	0	0	0.22(3)
Ca2	2c	1.0	0	1/2	0	0.43(9)
O1	4e	1.0	0.2164(13)	0.1810(13)	−0.0465(14)	1.08(12)
O2	4e	1.0	0.3232(14)	0.7193(13)	−0.0603(13)	1.08
O3	4e	1.0	0.3935(14)	−0.0423(11)	0.2307(10)	1.08

Table 2
Crystallographic data for Ca_2LuRuO_6

Atom	Site	Occupancy	*x*	*y*	*z*	B ($Å^2$)
Ca1	4e	0.965(1)	0.5151(1)	0.5556(3)	0.2508(5)	0.60(7)
Lu1	4e	0.035(1)	0.5151	0.5556	0.2508	0.60
Ru	2d	1.0	1/2	0	0	0.11(4)
Ca2	2c	0.071(1)	0	1/2	0	0.34(3)
Lu2	2c	0.929(1)	0	1/2	0	0.34
O1	4e	1.0	0.2194(15)	0.1922(15)	−0.0552(15)	0.26(11)
O2	4e	1.0	0.3167(15)	0.7184(14)	−0.0580(14)	0.26
O3	4e	1.0	0.3976(13)	−0.0375(12)	0.2358(12)	0.26

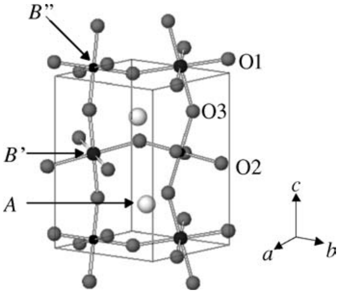

Fig. 2. The schematic crystal structure of Ca_2LnRuO_6 ($Ca_{2-x}Ln_x$ $[Ln_{1-x}Ca_x]RuO_6$); A = $Ca_{2-x}Ln_x$, B′ = $Ln_{1-x}Ca_x$ and B″ = Ru.

ever, they show the change in their slopes between Ln = Dy and Ho. In particular, the β parameter changes dramatically at the same border. Fig. 4 shows the variation of the occupancy x with the ionic radius of Ln^{3+} ions. It is revealed that the x value depends on the Ln^{3+} radius. For the compounds with Ln = La–Tb, the Ca^{2+} ion mainly occupies the B′ site. From Ln = Dy to Er, the Ca^{2+} ion is gradually replaced by the Ln^{3+} ion at the B′ site. When Ln = Tm, Yb and Lu, the B′ site is mainly occupied by the Ln^{3+} ion. This drastic change is agreement with that of lattice parameters.

The average Ru–O and ($Ln_{1-x}Ca_x$)–O bond lengths are plotted against the Ln^{3+} radius in Fig. 5. The Ru–O bond

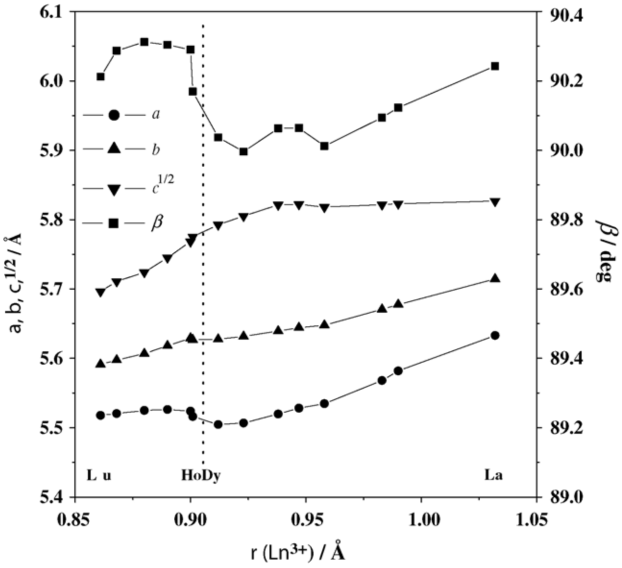

Fig. 3. Variation of lattice parameters for Ca_2LnRuO_6 with the six-coordinate ionic radius of Ln^{3+}.

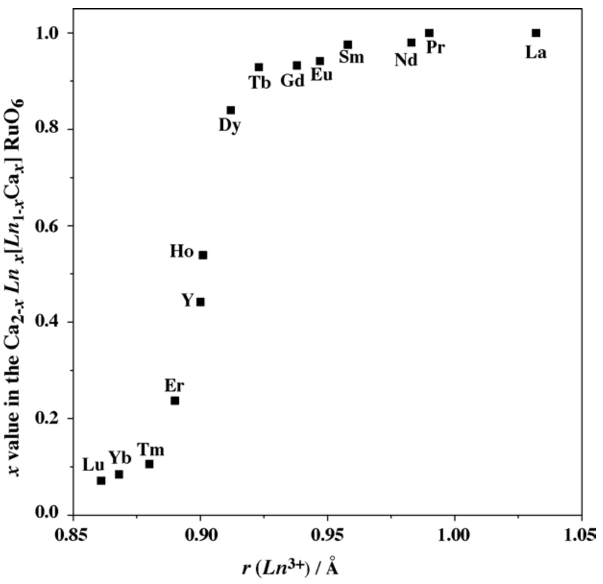

Fig. 4. The ratio of the Ca^{2+} at the B′ site.

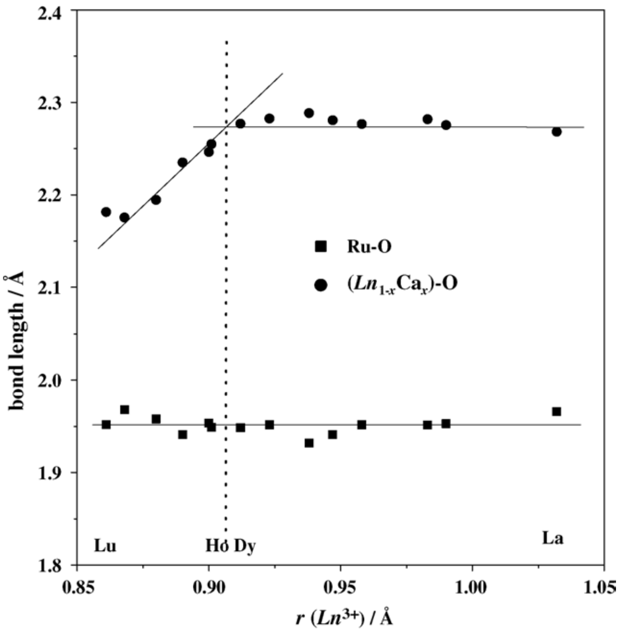

Fig. 5. Plots of average B′–O and B″–O bond lengths against the Ln^{3+} radius ($B' = Ln_{1-x}Ca_x$ and $B'' = Ru$).

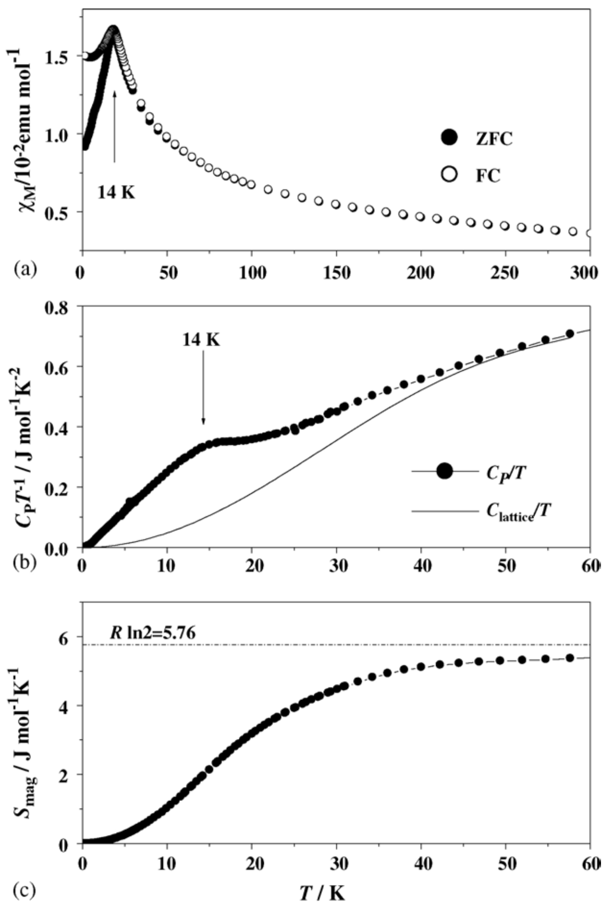

Fig. 6. (a) Temperature dependence of the susceptibilities for Ca_2LuRuO_6. Filled symbols (●) correspond to ZFC susceptibilities and open symbols (○) correspond to FC susceptibilities; (b) temperature dependence of the specific heat divided by temperature (C_P/T) for Ca_2LuRuO_6. The solid line represents the calculated lattice specific heat and (c) magnetic entropy for Ca_2LuRuO_6.

length is constant without depending on the ionic radius of Ln^{3+} ions and is in good agreement with the Ru^{5+}–O^{2-} distance calculated from the Shannon's ionic radii (1.965 Å) [11]. The $(Ln_{1-x}Ca_x)$–O bond length is constant from Ln = La to Dy, while it decreases with the decrease of Ln^{3+} ionic radius from Ho to Lu. This result corresponds to the fact that the Ca^{2+} is mainly occupied at the B′ site in the former case while the Ln^{3+} ion is mainly occupied at the B′ site in the latter case.

Previously, we have investigated A_2LnRuO_6 (A = Sr, Ba) and found that Sr^{2+} (or Ba^{2+}) and Ln^{3+} ions fully occupy the A and B′ sites, respectively. The ionic radii of the Sr^{2+} and Ba^{2+} ions in the six-coordination are 1.18 and 1.35 Å, respectively, and are much larger than that of Ln^{3+} (0.861 Å for Lu^{3+} and 1.032 Å for La^{3+}). The cation disorder of the B′ and A sites found in the Ca_2LnRuO_6 series is due to the fact that the ionic radius of Ca^{2+} (1.00 Å) is near to that of Ln^{3+}.

3.2. Magnetic properties

The molar magnetic susceptibilities of Ca_2LuRuO_6 are plotted as a function of temperature in Fig. 6(a). It is found that an antiferromagnetic transition occurs at $T_N = 14$ K. Its reciprocal magnetic susceptibility versus temperature curve was fitted with the Cutie–Weiss law in the temperature range between 100 and 300 K. The effective magnetic moment was obtained to be 3.18 μ_B. It is smaller than the spin-only value for the Ru^{5+} ion with $S = 3/2$. The large negative Weiss constant ($\theta = -104.9$ K) indicates that the predominant magnetic exchange interaction between Ru^{5+} ions is antiferromagnetic. The data of specific heat show an anomaly at 14 K (Fig. 6(b)). This temperature agrees with the magnetic transition temperatures observed in the magnetic susceptibility. To calculate the magnetic contribution to the specific heat, we have to subtract the lattice, electronic and nuclear specific heat contribution from the total specific heat. They were estimated by using a polynomial function of the temperature, $f(T) = aT^3 + bT^5 + cT^7$ [12], in which the constants were determined by fitting this function to the observed specific heat data between 50 and 60 K. From the temperature dependence of the magnetic specific heat, the magnetic entropy change of Ca_2LuRuO_6 is calculated as shown in Fig. 6(c). The magnetic entropy change due to the antiferromagnetic ordering of Ru^{5+} ions in the Ca_2LuRuO_6 is about 5 J mol^{-1} K^{-1}. The magnetic entropy change of Ru^{5+} is calculated to be $R\ln(2S+1) = 11.5$ J mol^{-1} K^{-1}, where R and S are the molar gas constant and the spin quantum number, respectively. In an octahedral crystal field environment, the ground state of the Ru^{5+} ion ($4d^3$, the state $^4F_{3/2}$) is the four-fold degenerate state. In the case of lower symmetry, this state splits into two Kramers doublet states. For such a case, the magnetic entropy change is $R\ln 2 = 5.76$ J mol^{-1} K^{-1}. The result of the magnetic entropy change indicates that the degeneracy of the ground state for the Ru^{5+} ion in Ca_2LuRuO_6 should be doublet.

References

[1] Y. Izumiyama, Y. Doi, M. Wakeshima, Y. Hinatsu, A. Nakamura, Y. Isii, J. Solid State Chem. 169 (2002) 125.
[2] Y. Izumiyama, Y. Doi, M. Wakeshima, Y. Hinatsu, Y. Shimojo, Y. Morii, J. Phys.: Condens. Matter 13 (2001) 1303.
[3] Y. Doi, Y. Hinatsu, K. Oikawa, Y. Shimojo, Y. Morii, J. Mater. Chem. 10 (2000) 797.
[4] Y. Doi, Y. Hinatsu, J. Phys.: Condens. Matter 11 (1999) 4813.
[5] P.D. Battle, C.W. Jones, J. Solid State Chem. 78 (1989) 108.
[6] P.D. Battle, W.J. Macklin, J. Solid State Chem. 52 (1984) 138.
[7] P.D. Battle, W.J. Macklin, J. Solid State Chem. 54 (1984) 245.
[8] P.D. Battle, J.B. Goodenough, R. Price, J. Solid State Chem. 46 (1983) 234.
[9] P.D. Battle, C.W. Jones, F. Studer, J. Solid State Chem. 90 (1991) 302.
[10] F. Izumi, T. Ikeda, Mater. Sci. Forum 321–324 (2000) 198.
[11] R.D. Shannon, Acta Crystallogr. A 32 (1976) 751.
[12] J.E. Gordon, R.A. Fisher, Y.X. Jia, N.E. Phillips, S.F. Reklis, D.A. Wright, A. Zettl, Phys. Rev. B 59 (1999) 127.